Metabolic Engineering 24 (2014) 129–138

Contents lists available at ScienceDirect

Metabolic Engineering

journal homepage: www.elsevier.com/locate/ymben

Model based engineering of *Pichia pastoris* central metabolism enhances recombinant protein production

Justyna Nocon [a], Matthias G. Steiger [a,d], Martin Pfeffer [a,1], Seung Bum Sohn [b], Tae Yong Kim [b], Michael Maurer [c,d], Hannes Rußmayer [a,d], Stefan Pflügl [a,d], Magnus Ask [a,d], Christina Haberhauer-Troyer [d,e], Karin Ortmayr [e], Stephan Hann [d,e], Gunda Koellensperger [d,e], Brigitte Gasser [a,d], Sang Yup Lee [b,f], Diethard Mattanovich [a,d,*]

[a] Department of Biotechnology, University of Natural Resources and Life Sciences Vienna, Muthgasse 18, Vienna, Austria
[b] Bioinformatics Research Center, Korea Advanced Institute of Science and Technology (KAIST), Daejeon, Republic of Korea
[c] School of Bioengineering, University of Applied Sciences FH Campus Wien, Vienna, Austria
[d] Austrian Centre of Industrial Biotechnology, Vienna, Austria
[e] Department of Chemistry, University of Natural Resources and Life Sciences, Vienna, Austria
[f] Metabolic Engineering National Research Laboratory, Department of Chemical and Biomolecular Engineering (BK21 plus program), BioProcess Engineering Research Center, Center for Systems and Synthetic Biotechnology, KAIST Institute for the BioCentury, Korea Advanced Institute of Science and Technology (KAIST), Daejeon, Republic of Korea

ARTICLE INFO

Article history:
Received 20 January 2014
Received in revised form
9 May 2014
Accepted 12 May 2014
Available online 20 May 2014

Keywords:
Metabolic modeling
GEM
Recombinant protein
Yeast
Flux analysis
NADPH

ABSTRACT

The production of recombinant proteins is frequently enhanced at the levels of transcription, codon usage, protein folding and secretion. Overproduction of heterologous proteins, however, also directly affects the primary metabolism of the producing cells. By incorporation of the production of a heterologous protein into a genome scale metabolic model of the yeast *Pichia pastoris*, the effects of overproduction were simulated and gene targets for deletion or overexpression for enhanced productivity were predicted. Overexpression targets were localized in the pentose phosphate pathway and the TCA cycle, while knockout targets were found in several branch points of glycolysis. Five out of 9 tested targets led to an enhanced production of cytosolic human superoxide dismutase (hSOD). Expression of bacterial β-glucuronidase could be enhanced as well by most of the same genetic modifications. Beneficial mutations were mainly related to reduction of the NADP/H pool and the deletion of fermentative pathways. Overexpression of the hSOD gene itself had a strong impact on intracellular fluxes, most of which changed in the same direction as predicted by the model. *In vivo* fluxes changed in the same direction as predicted to improve hSOD production. Genome scale metabolic modeling is shown to predict overexpression and deletion mutants which enhance recombinant protein production with high accuracy.

1. Introduction

Heterologous protein production is a multi-billion dollar market, mainly covering biopharmaceuticals and industrial enzymes. Microbial production systems, like bacteria and yeasts, are in many cases characterized by high synthesis rates and product titers (Porro et al., 2011). Nevertheless, there are still limits in productivity observed. In particular, a negative impact of recombinant protein production on cell growth is observed which has to be attributed to more than just a stoichiometric drain of energy from biomass formation towards product formation. In yeast systems, these limitations are ascribed to bottlenecks in protein folding and secretion in case of secretory proteins (recently reviewed by Idiris et al., (2010) and Damasceno et al., (2012), limited transcriptional efficiency due to weak promoters or low gene copy numbers (reviewed in Gasser et al., 2013) or to intracellular proteolytic degradation (Pfeffer et al., 2011). Additionally, metabolic limitations cannot be ruled out as a cause for suboptimal productivity of heterologous proteins (Heyland et al., 2011a; Heyland et al., 2011b; Kaleta et al., 2013; Klein et al., 2014; Kazemi Seresht et al., 2013). To address this problem, metabolic modeling can be applied for

* Corresponding author at: Department of Biotechnology, University of Natural Resources and Life Sciences, Muthgasse 18, Vienna, Austria.
E-mail address: diethard.mattanovich@boku.ac.at (D. Mattanovich).
[1] Current address: ERBER AG, Tulln, Austria.

http://dx.doi.org/10.1016/j.ymben.2014.05.011

both computational simulation of metabolic flux networks and experimental flux analyses. These analyses are then employed to predict targets for metabolic engineering to enhance productivity (Xu et al., 2013).

Vijayasankaran et al., (2005) showed that the amino acid composition of heterologous proteins has a profound impact on the predicted elementary flux modes leading to high protein production in *Escherichia coli*. Oddone et al., (2009) have used a dynamic flux balance analysis model to predict targets for gene downregulation to enhance production of recombinant green fluorescent protein (GFP) in *Lactococcus lactis*. Knock down of two of the predicted genes led to a 15% increase of GFP per cell mass. Furthermore, the process of protein synthesis is highly energy demanding. Consequently higher intracellular ATP levels should enhance the cellular capacity to produce recombinant proteins, as it was shown for *E. coli* (Kim et al., 2012).

Overexpression of a recombinant (in this case homologous) enzyme in *Aspergillus niger* led to significant changes in metabolic flux distribution, mainly enhancing reactions towards NADPH production and reducing the tricarboxylic acid (TCA) cycle flux (Driouch et al., 2012). Comparing the *in vivo* flux distribution with theoretical flux distributions calculated by elementary mode analysis revealed that the metabolism was already shifted to a large extent towards optimum flux distribution just by overproduction of the recombinant protein. The same pattern of flux changes was also observed for *Aspergillus oryzae* overproducing α-amylase (Pedersen et al., 1999).

The yeast *Pichia pastoris* is well established as a host for the production of heterologous proteins (Gasser et al., 2013). Recombinant overexpression of heterologous proteins in *P. pastoris* was shown to increase TCA cycle flux and ATP production slightly (Dragosits et al., 2009; Heyland et al., 2010). *De novo* synthesis of amino acids, in particular the synthesis of energetically costly ones, was identified as a limiting metabolic process for protein overproduction (Heyland et al., 2011b).

Genome sequencing of *P. pastoris* (Mattanovich et al., 2009; De Schutter et al., 2009) laid the basis for establishing genome-scale metabolic models (GEM) of this yeast (Sohn et al., 2010; Chung et al., 2010; Caspeta et al., 2012). The incorporation of heterologous protein production into the metabolic model allowed the investigation of the interplay among protein production, energy demand and biomass formation (Sohn et al., 2010). In the present work we aimed to verify predicted flux changes caused by protein overproduction by ^{13}C labeling based flux analysis, and to employ the GEM to predict beneficial mutations in the *P. pastoris* central carbon metabolism. The model was used to predict gene knock out targets by Minimization of Metabolic Adjustment (MOMA) and overexpression targets by Flux Scanning based on Enforced Objective Function (FSEOF) for enhanced production of intracellular human copper/zinc superoxide dismutase (hSOD). We present the effects of manipulating central metabolic fluxes on the production of hSOD in *P. pastoris*.

2. Materials and methods

2.1. Strains and vectors

The *P. pastoris* strains used in this study were based on the wild type strain X-33 (Invitrogen). The strain producing intracellular human superoxide dismutase under control of the strong glycolytic glyceraldehyde-3-phosphate dehydrogenase (GAP) promoter (X-33_hSOD_NTS), carrying 15 copies of the hSOD gene was described by Marx et al. (2009). For production of intracellular β-glucuronidase A (GusA) from *E. coli* (Jefferson et al., 1986), the respective gene was cloned into the *P. pastoris* Puzzle vector (Stadlmayr et al., 2010) and integrated into the *P. pastoris* genome into the *AOX1* terminator locus.

E. coli strain top 10 (invitrogen) was used as a DNA manipulation host.

2.2. Cultivation of P. pastoris

For metabolic flux analysis cells were grown at 25 °C in 50 mL of YNB medium (3.4 g L^{-1} YNB w/o amino acids and ammonia sulfate, 10 g L^{-1} $(NH_4)_2SO_4$, 400 mg L^{-1} biotin, 20 g L^{-1} glucose) in 250 mL wide neck shake flasks without baffles. For ^{13}C labeling glucose was a mixture of 17% uniformly labeled ^{13}C glucose and 83% naturally labeled glucose. The cells were inoculated at an OD = 0.03 and grown until exponential phase (OD around 1). Glucose uptake and extracellular metabolites were determined in cultures grown on YNB with unlabeled glucose.

For determination of hSOD production, strains were cultivated at 25 °C in 10 mL YPD medium supplemented with 2 mM $CuCl_2$ and 0.02 mM $ZnSO_4$ in 100 mL wide neck shake flasks without baffles. The cultures were grown for 48 h and fed three times in 12 h intervals with 100 μL of 50 g L^{-1} glucose solution. GusA production was determined in cultures grown in minimal medium as described by Gasser et al. (2013), cultivated as above.

Optical density was measured at 600 nm wavelength in 1 mL of culture broth using a WPA CO8000 Cell Density Meter. For determination of yeast dry mass (YDM) 9 mL of culture broth was centrifuged, washed with 10 mL of ddH_2O and dried for 24 h at 105° in preweighed tubes. YDM was then related to OD to calculate biomass concentrations. Unless described differently all cultures were repeated in triplicate.

2.3. Recombinant protein quantification

At the end of the cultivation, 1 mL aliquots of cells were harvested and wet cell weight was determined. For further analysis the cell pellets were kept at −20 °C. The harvested cell pellets were re-suspended in 500 μL extraction buffer (20 mM Tris–HCl pH 8.2, 5 mM EDTA, 0.1% Triton X-100, 7 mM β-mercaptoethanol, 1 mM $CuCl_2$, 0.1 mM $ZnSO_4$ and protease inhibitor cocktail (Sigma)) and mechanically disrupted with 500 μL glass beads (diameter 0.5 mm) on a FastPrep® in 3 cycles of 20 s at 6.5 m s^{-1} and 5 min rest on ice. The hSOD concentration in the cell extracts was determined by ELISA (Marx et al., 2009) and correlated with total protein content (determined by Coomassie Protein Assay, Thermo Scientific).

For GusA determination the cell pellets were re-suspended in an extraction buffer (100 mM sodium phosphate buffer pH 7.0, 2 mM EDTA, 0.02% Triton X-100, 10 M DTT) and mechanically disrupted with glass beads as described above. The GusA concentration in the cell extracts was determined by 4-methylumbelliferyl-β-d-glucuronide (MUG) activity assay as described by Blumhoff et al. (2013).

2.4. Metabolic flux analysis

^{13}C labeling patterns of protein-bound amino acids were analyzed with GC–MS according to Zamboni et al. (2009) using an Agilent 6890N gas chromatograph coupled to a 5975 mass spectrometer equipped with a Phenomenex Zebron ZB-5MS column (30 m × 0.25 mm i.d. × 0.25 μm film thickness). In order to improve the selectivity of histidine detection the original temperature program was modified as follows: 160 °C for 1 min, with 20 °C/min to 250 °C, with 5 °C/min to 270 °C, with 30 °C/min to 310 °C, hold for 0.5 min.

Specific growth rates, glucose uptake rates and metabolite secretion rates were determined during the exponential growth phase between 17 and 23 h after inoculation.

Flux calculations were performed with OpenFLUX using standard settings and applying the gradient based search algorithm for sensitivity analysis (Quek et al., 2009). The stoichiometric model (provided in the supplementary file) was based on a previously published *P. pastoris* model of the central carbon metabolism (Baumann et al., 2010). Uptake and secretion rates of extracellular metabolites were measured by HPLC. The biomass composition of *P. pastoris* wild type strain X-33 and recombinant protein expressing strains were determined previously. For the hSOD-expressing strain the composition as for the Fab-expressing strain was assumed (Carnicer et al., 2009). Mass distribution vectors of amino acids were extracted from GC–MS raw data using FiatFlux (Zamboni et al., 2005). Mass distribution values are provided in the supplementary file.

2.5. Analysis of intracellular $NADP^+$ and NADPH

The protocol for extraction of $NADP^+$ and NADPH from cell pellets was adapted from the works of Canelas et al., (2009). One milliliter samples of 24 h grown cultures were centrifuged and the cell pellets were extracted in 1 mL of 5 mM ammonium acetate (pH 8.0) for 3 min at 85 °C with intermediate mixing. After centrifugation, supernatants were separated on a silica-based C18 column (Waters Atlantis T3, 2.1 × 150 mm^2, 3 μm). The HPLC system (Thermo Accela 1250) was coupled to a triple quadrupole MS system (Thermo TSQ Vantage) via a heated ESI ion source for quantification. As described by Ortmayr et al., (2014) an absolute quantification of NADPH is limited by its rapid oxidation and the lack of an isotopically labeled standard to compensate for losses during sample preparation. However relative quantification can be achieved reproducibly. NADPH was also measured in the same samples with the enzymatic cycling assay as described by Ask et al. (2013) showing the same relative NADPH levels.

2.6. Prediction of knockout and overexpression targets

Identification of gene overexpression targets for increasing recombinant protein production was performed using Flux Scanning based on Enforced Objective Function (FSEOF) (Choi et al., 2010) using the GEM of Sohn et al. (2010). Gene targets that were selected showed increased flux through their respective metabolic reactions when an increased flux towards protein production was enforced as an additional constraint to the metabolic model.

Identification of gene knockouts was performed with Minimization of Metabolic Adjustment (MOMA) (Segrè et al., 2002). Six gene knockout targets were selected that showed minor decrease in biomass production and an increase in specific protein synthesis.

2.7. Overexpression of target genes

The target genes for overexpression were amplified from X-33 genomic DNA and cloned under control of the GAP promoter into the Puzzle vector (Stadlmayr et al., 2010) containing a HphMX (hygromycin) resistance cassette. Primers are given in the supplementary file. The vectors were integrated into the *AOX1* terminator locus of the *P. pastoris* genome.

2.8. Knock out of target genes

The genes predicted as knock out targets were disrupted using the split marker cassette method established recently for *P. pastoris* (Heiss et al., 2013). Thereby, two fragments of 700 bp, one located around 200 bp upstream of the start codon and one located around 200 bp downstream of the start codon of the respective genes, were used to flank the HphMX resistance cassette. Upon transformation, the homologous recombination event replaces a 5′ fragment of the gene and its promoter with the antibiotic resistance. To increase the gene-targeting efficiency, the resistance gene is split into two overlapping fragments, which can only integrate into the host genome upon a successful homologous recombination event. For the verification of gene knockouts, genomic DNA of the modified strains was isolated on FTA™ cards (Whatmann) and used for PCR with primers located outside of the split marker cassette, where positive transformants give an approximately 1000 bp larger fragment compared to the wild type. All primers are given in the supplementary file.

2.9. Enzyme activity assays

Strains overexpressing glucose-6-phosphate dehydrogenase (*ZWF1*) and malate dehydrogenase (*MDH1*) were screened for the respective enzyme activity. The glucose-6-phosphate dehydrogenase assay was performed according to Souza et al. (2002). Briefly, cells were mechanically disrupted with glass beads, and the cell extracts were added to the reaction buffer (100 mM Tris–HCl pH = 7.5) containing 3 mM $MgCl_2$, 0.2 mM $NADP^+$ and 4 mM glucose-6-phosphate. Reduction of $NADP^+$ was followed by the increase of absorbance at 340 nm in 30 s intervals over 6 min using a spectrophotometer.

Malate dehydrogenase activity was measured according to (McAlister-Henn and Thompson, 1987) by addition of the cell extracts to reaction buffer (100 mM imidazol, 200 mM KCl, 2 mM EDTA, 10 mM $MgSO_4 \cdot 7H_2O$) containing 0.3 mM NADH and 100 mM oxaloacetate. The oxidation of NADH corresponding to decrease in the absorbance at 340 nm was followed in 30 s intervals for 6 min.

2.10. Analysis of external metabolites

To measure external metabolites the strains were cultivated as for ^{13}C labeling in liquid cultures with a starting OD = 0.1 until a stationary phase was reached. Sampling was performed every 12 h. At each time point optical density of the culture was measured and supernatant was collected for measurement of external metabolites. Glucose, ethanol, arabitol, acetate, acetaldehyde and pyruvate were quantified by HPLC analysis, as described by Pflügl et al. (2012) using a Rezex ROA-Organic Acid H^+ 300 mm × 7.8 mm column (Phenomenex, USA).

3. Results and discussion

3.1. Effect of hSOD overexpression on predicted and measured metabolic fluxes

In a previous study we correlated enhanced hSOD production with high gene copy number of hSOD expression cassettes. The best hSOD strain produced 4 mg g^{-1} hSOD per dry biomass, reaching 272 mg L^{-1} hSOD in fed batch (Marx et al., 2009). However, overproduction of hSOD led to a decrease of biomass yield to 75% of the wild type strain, yielding lower biomass formation in strains with higher hSOD productivity, as observed for other heterologous proteins in different hosts too. Significant intracellular flux changes between wild-type and hSOD strain were predicted by the GEM. To verify these flux changes experimentally, we performed flux analysis of the hSOD strain and the X-33 control strain based on ^{13}C labeling in unlimited batch cultures (which resemble the simulations of the GEM). Metabolic fluxes of both strains are shown in Fig. 1. In the wild type strain, the split ratio between glycolysis and PPP was 0.72 to 0.28. From the pyruvate node, 5% are directed to the fermentative pathway,

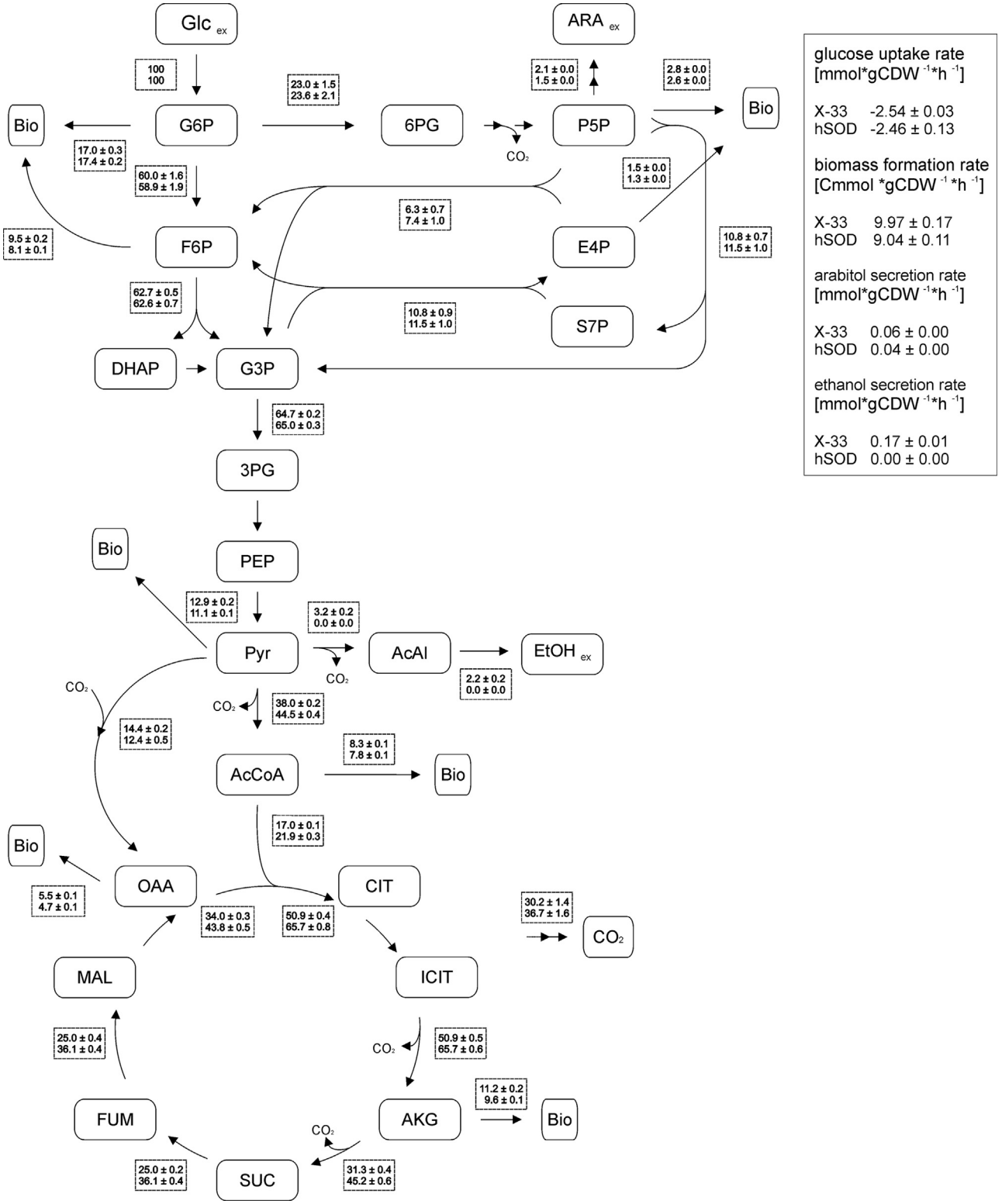

Fig. 1. Flux distribution in strains X-33 and hSOD. The flux values are normalized to glucose uptake and presented in [% Cmol]. The upper value in the rectangular boxes represents the flux distribution of strain X-33 and the lower value the flux distribution of hSOD strain. For reversible reactions only the net fluxes are presented.

75% to the TCA cycle and 20% to biomass. The PPP flux in the hSOD strain was slightly higher than in the wild type strain (although statistically not significant). TCA flux increased by 29%, and the fermentative branch through pyruvate decarboxylase decreased below the detection limit in the hSOD strain.

The production of hSOD leads to an increase of the total NADP/H pool as well as the NADPH concentration, so that the anabolic reduction charge is increased almost threefold (Table 1). Protein production requires anabolic reductive power for the synthesis of amino acids. Apparently the extra demand is compensated in the hSOD strain by the observed changes in the NADP/H pool.

The predicted flux changes of hSOD *vs.* X-33 strain showed mainly the same trends as the actually measured flux changes.

Table 1
Total NADP/H pools and relative anabolic reduction charge of strains X-33, hSOD, ZWF1 and SOL3. SEM=standard error of the mean. FC=fold change.

Strain	NADP/H pool (μmol/g YDM)	SEM	Relative reduction charge (FC to X-33)	SEM
X-33	0.38	0.025	1.0	0.52
SOD	0.55	0.040	2.9	0.64
ZWF1	0.49	0.002	3.1	0.03
SOL3	0.58	0.029	1.6	0.30

In the hSOD strain, mainly the TCA flux increases, while PPP and glycolytic fluxes remain almost unchanged, and the fermentative branches to ethanol and arabitol decrease in the production strain. While directions of flux changes are well predicted the model underestimates the change in TCA flux. The GEM predicted a higher PPP flux in the hSOD strain indicating a higher demand of NADPH in this strain. The PPP flux increased only slightly in the hSOD strain, but the total NADP/H concentration and the fraction of the reduced form increased in this strain. Driouch et al. (2012) have observed a similar overlap of predicted flux changes upon overproduction of recombinant fructofuranosidase in *A. niger*. They employed elementary flux mode calculation to predict fluxes, and found a 63% overlap of measured flux changes with the prediction. An increase of PPP flux was observed, while TCA cycle flux decreased in the *A. niger* overproduction strain. A very similar pattern was also observed with *A. oryzae* producing recombinant α-amylase (Pedersen et al., 1999), with *Schizosaccharomyces pombe* overproducing maltase (Klein et al., 2014) and with *S. cerevisiae* producing human SOD (Gonzalez et al., 2003). An increase of TCA cycle flux was observed here and consistently before in *P. pastoris* strains producing different recombinant proteins (Dragosits et al., 2009; Heyland et al., 2011b; Jordà et al., 2012). A literature review reveals an increased TCA flux attributed to higher energy demand also in *E. coli* (Weber et al., 2002) and CHO cells (Sheikholeslami et al., 2013) during recombinant protein production. In contrast, a decreased TCA flux was also observed in *E. coli* (Wittmann et al., 2007). Especially the latter case shows that this effect is not only host species dependent but also related to the produced protein. While Klein et al. (2014) describe a downregulation of TCA cycle flux in recombinant *S. pombe*, they observed an increase of recombinant maltase production when TCA cycle was enforced by a substrate change. We conclude that increased energy production by enhanced TCA cycle flux is an important prerequisite for recombinant protein production. However, the ability to shift the metabolism towards enhanced energy production depends obviously both on the host organism and specific features of the produced protein and the production strain.

3.2. Prediction of overexpression and knockout targets

The GEM by Sohn et al. (2010) was used for prediction of metabolic engineering targets beneficial to hSOD production. Nine metabolic reactions were predicted by FSEOF to enhance hSOD productivity upon their overexpression (Table 1). They include 6 consecutive steps of the pentose phosphate pathway (PPP) (*ZWF1*, *SOL3*, *GND2*, *RPE1*, *TKL1* and *TAL1*), two genes related to the TCA cycle (*MDH1* and *GDH3*), and *GPD1* of the glycerol pathway. To visualize the affected pathways all these reactions are indicated in Fig. 2.

Prediction of beneficial single gene knockouts with MOMA (Fig. 3) led to 6 targets (Table 2), mainly related to the fermentative pathway downstream of the pyruvate nodes (*PDC1*, *ADH2*, *ALD4* and *PDA1*), to glycolysis (*TPI1*) and to the glycerol pathway (*GUT2*). Most of these knockouts may increase the pyruvate pool and will thus lead to an increase of the TCA cycle flux (with the exception of *PDA1*). *GUT2* knockout may increase the glycerol pool by reducing its degradation. These proposed knockouts are visually presented in Fig. 2.

The predicted overexpressions in the upper part of the PPP and of *GDH3* are directly related to the reduction of $NADP^+$. Also a potential deletion of *TPI1* should enhance the oxidative part of the PPP and thus NADPH levels (Krüger et al., 2011). *De novo* synthesis of proteins costs both energy and reduction equivalents

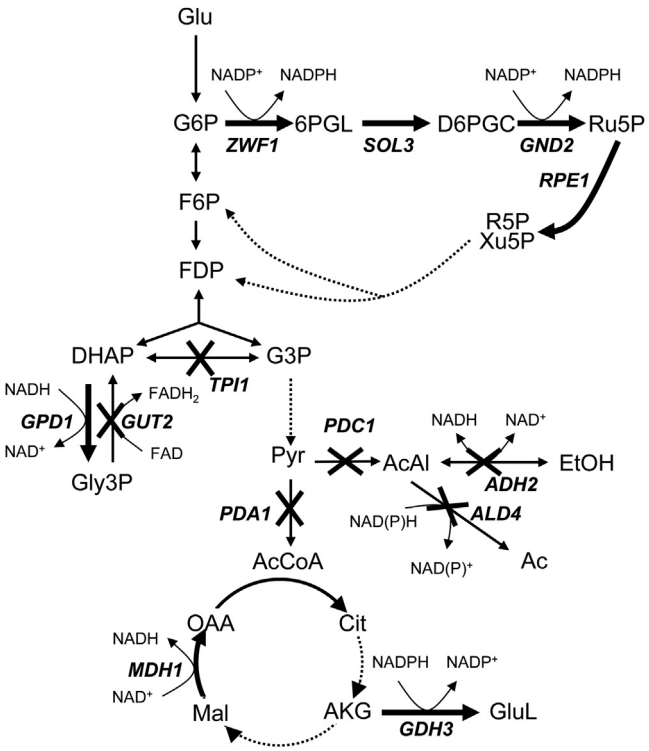

Fig. 2. Overexpression (OE) and knockout (KO) targets illustrated in the metabolic map of the central metabolism. The targets for single gene KO and OE are indicated by their gene names. OE targets are illustrated by a thick arrow, and KO targets by a crossed reaction. Turnover of redox cofactors is shown for the selected reactions.

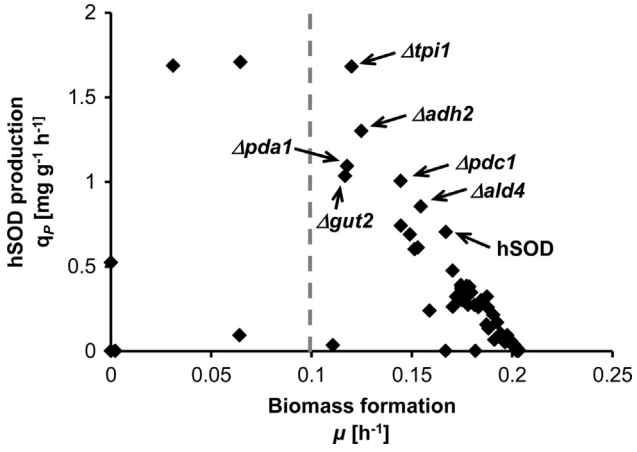

Fig. 3. Simulation results for single gene knockout targets using MOMA to increase the production of hSOD. A cut-off value of 0.1 h^{-1} was used for the biomass formation (dashed line), to select mutants that are capable of achieving increased hSOD production while at the same time, do not greatly inhibit growth. The base strain expressing hSOD production and the top knockout candidates are pointed out with their respective gene names. (Δ*adh2*: alcohol dehydrogenase, Δ*ald4*: aldehyde dehydrogenase, Δ*gut1*: glycerol-3-phosphate dehydrogenase, Δ*pda1*: pyruvate dehydrogenase, Δ*pdc1*: pyruvate decarboxylase, Δ*tpi1*: triose-phosphate isomerase).

Table 2
Predicted knockout (MOMA) and overexpression (FSEOF) targets for increased production of hSOD.

Genes	Enzyme names	Gene name	$\log_2$ flux change hSOD/X-33
MOMA target			
PIPA03164 PIPA01726	Pyruvate decarboxylase	*PDC1*	$\ll -5$
PIPA03313 PIPA02544	Alcohol dehydrogenase (ethanol)	*ADH2*	$\ll -5$
PIPA00390	Aldehyde dehydrogenase (acetylaldehyde, NAD)	*ALD4*	n.d.*
PIPA02794 PIPA03785 PIPA04299 PIPA03623	Pyruvate dehydrogenase	*PDA1*	0.23 ± 0.02
PIPA03441	Triose-phosphate isomerase	*TPI1*	0.00 ± 0.03
PIPA02567	Glycerol-3-phosphate dehydrogenase (FAD)	*GUT2*	0.00 ± 0.03
FSEOF target			
PIPA08178	Glucose 6-phosphate dehydrogenase	*ZWF1*	0.04 ± 0.23
PIPA04435	6-phosphogluconolactonase	*SOL3*	0.04 ± 0.23
PIPA03124	Phosphogluconate Dehydrogenase	*GND2*	0.04 ± 0.23
PIPA03251	Ribulose 5-phosphate 3-epimerase	*RPE1*	-0.15 ± 0.02
PIPA02093	Transketolase	*TKL1*	0.09 ± 0.22
PIPA03744	Transaldolase	*TAL1*	0.09 ± 0.22
PIPA06084	Glycerol-3-phosphate dehydrogenase	*GPD1*	0.01 ± 0.02
PIPA02244	Malate dehydrogenase	*MDH1*	0.56 ± 0.01
PIPA03564	Glutamate dehydrogenase (NADP)	*GDH3*	n.d.*

* Not determined.

(Kaleta et al., 2013). Heyland et al. (2011b) have shown that metabolically costly amino acids constitute a bottleneck in the production of recombinant aminopeptidase in *P. pastoris*. As the synthesis of these amino acids requires reduced NADPH a benefit of the enhanced reduction of the NADP/H pool on recombinant protein production appears plausible.

The benefit of other predicted mutations requires more in-depth analysis to be fully understood. Deletion of genes encoding reactions from pyruvate towards ethanol or acetate may lead to an increased TCA cycle flux and hence increased energy production, which may counteract the increased energy demand for synthesis of amino acids and recombinant protein. Actually it has been shown that recombinant protein production deviates the cellular metabolism of *P. pastoris* towards the TCA cycle (Dragosits et al., 2009; Heyland et al., 2011b; Jordà et al., 2012). The appearance of pyruvate dehydrogenase (*PDA1*) as a knockout target seems contradictory to overexpression targets of TCA cycle enzymes, as it is the entry point of carbon flux into the TCA cycle. To determine how *PDA1* can be a knockout target, we re-examined the flux in the GEM under the condition of *PDA1* deletion. It was found that in the *PDA1* mutant, the flux from pyruvate to acetyl-CoA can be re-routed through acetaldehyde to acetate, which is then converted to acetyl-CoA. This physiological state, however, was not reproduced experimentally, as the *PDA1* mutant strain was determined to be not viable (see Section 3.3).

The benefits of a decrease of fermentation ($\Delta pdc1$, $\Delta adh2$) and an increased TCA cycle flux (*MDH1*) on hSOD production were anticipated already in the hSOD strain. While the predicted gene overexpressions correlated to an increased flux through the respective reaction, the predicted gene deletions were mirrored by down regulation of the respective flux compared to the wild type (Table 2). The PPP flux increase in the hSOD strain however was not significant indicating that a further benefit on recombinant protein production should be achievable by overexpressing genes encoding PPP enzymes as proposed by the model.

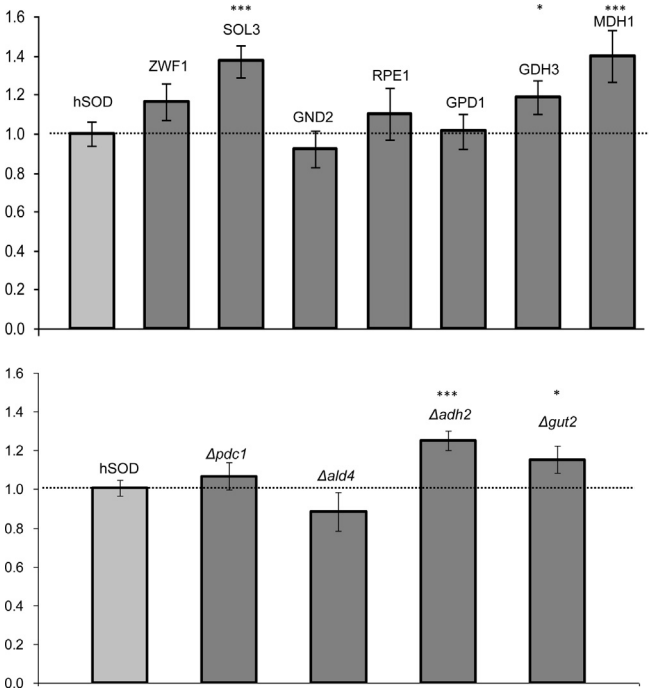

Fig. 4. Impact of mutations on hSOD expression levels. Relative changes of hSOD yield (μg hSOD per mg of total extracted proteins, relative to the hSOD control strain) are indicated. Data are means of 10 independent overexpression clones (upper panel) or 8 independent cultures of a knockout clone (lower panel), respectively. Error bars indicate the standard errors of the mean. Significance of differences to the control was calculated with Student's *t*-test. ***p-value < 0.01; *p-value < 0.1.

3.3. Gene knockout and overexpression in the hSOD strain

To study the impact of the model-predicted engineering targets on recombinant protein production, most of the aforementioned genes (Table 2) were overexpressed or knocked out, in the hSOD producing parental strain. Out of 6 predicted knockout targets, the deletion of pyruvate dehydrogenase subunit α (*PDA1*) and triose-phosphate isomerase (*TPI1*) were not achieved and thus assumed to be inviable under the tested conditions. Overexpression of 7 genes was performed, including the four consecutive steps of the upper oxidative part of the PPP, the two genes related to the TCA cycle, and *GPD1*. *TKL1* and *TAL1* were not selected due to uncertainties of their annotation.

Knockouts were verified by PCR, while enhanced activities of selected overexpressions (*ZWF1* and *MDH1*) were proven by enzymatic assays (data not shown).

3.4. Comparison of engineered strains and the parental hSOD strain

Overexpression targets were evaluated in 10 clones per strain, while each knockout was tested in 8 replicates per strain. The effect of cell engineering on recombinant protein production varied among the different mutant strains (Fig. 4). Among the 4 overexpressed PPP genes, *SOL3* had the strongest impact on hSOD production, leading to 40% increase in the produced protein. A beneficial effect was also seen by overexpression of *ZWF1*, the initial enzyme of the PPP, while no significant effect was seen by overexpression of the two latter PPP enzymes. Increased hSOD production was also observed upon *MDH1* overexpression (plus 40%) and to a lesser extent by *GDH3* overexpression. Out of the 4 knockout strains, an average of 1.2 fold higher hSOD levels could be detected in the Δ*adh2* strain. Most of the other strains showed minor positive effects.

It has to be noted that overexpression of single genes of a linear pathway may be suited to enhance the flux if the respective step has a major role in controlling this flux (Fell, 1998). Glucose-6-phosphate dehydrogenase (*Zwf1*) as the entry point of PPP should be the most plausible controlling step for the competition with the upper glycolytic pathway. In *S. cerevisiae* Zwf1 is regulated by the NADPH/$NADP^+$ ratio (Zubay, 1988) which would explain that overexpression of this enzyme has only a limited capacity to enhance the PPP flux. It was shown recently that the second step of the PPP, 6-phosphogluconolactonase (Sol3 and Sol4 in *S. cerevisiae*) is controlled both at the transcriptional and translational level in this yeast (Castelli et al., 2011; Zampar et al., 2013). Flux control analysis supports the claim that 6-phosphogluconolactonase is the major PPP flux controlling step in yeast (Messiha et al., 2014). A similar regulation of PPP enzymes can also be assumed in *P. pastoris*, as reflected by the increases in hSOD production by overexpression of Sol3 and Zwf1. Regarding TCA cycle, Driouch et al. (2012) propose an attenuation or knockout of malate dehydrogenase in *A. niger* to further improve protein production (awaiting experimental verification), which stands in contrast to the actual benefit of an overexpression of this gene in *P. pastoris*, as shown here. There is no clear connection identified between Mdh1 activity and protein synthesis, and the difference between *A. niger* and *P. pastoris* may be associated with the opposite changes of the TCA cycle flux in these two species.

A second intracellular model protein, GusA, was chosen to verify the effect of the model predictions on protein production. The majority of beneficial effects of mutations in the central carbon

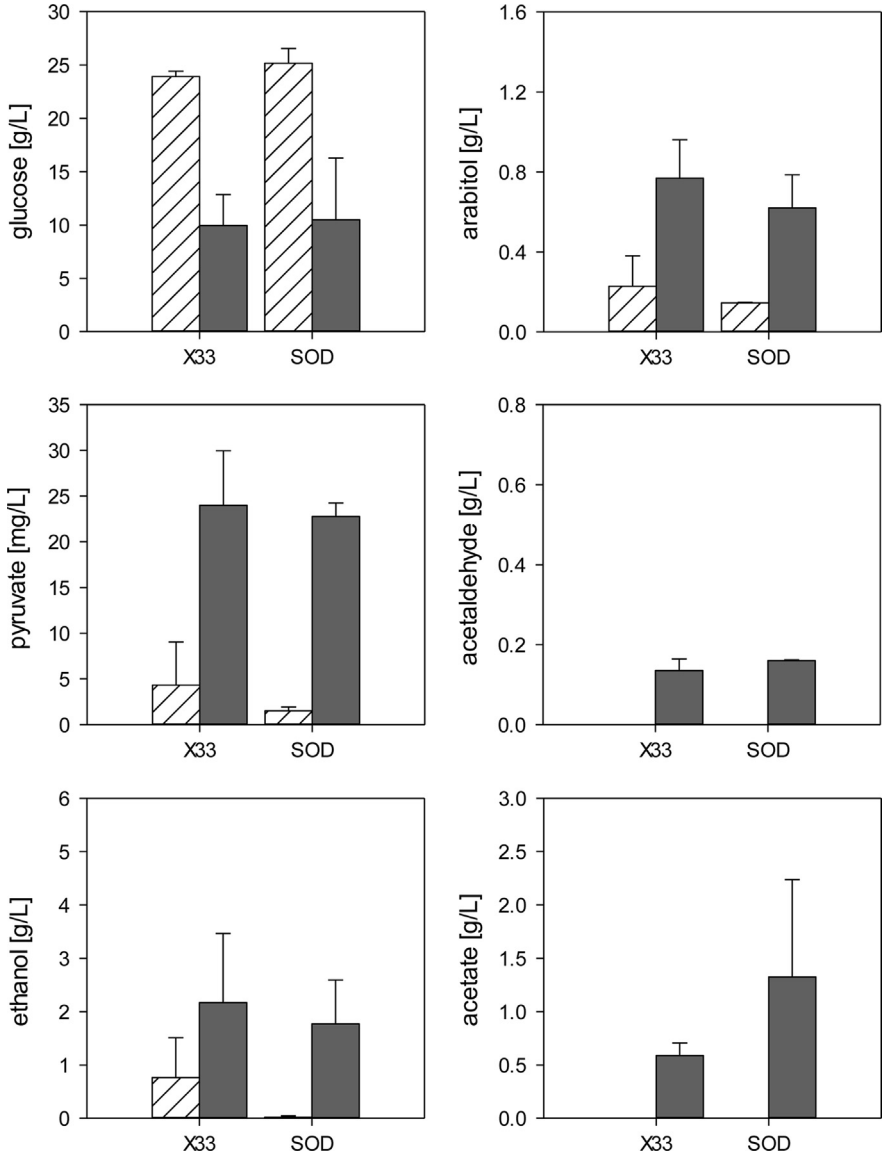

Fig. 5. Extracellular metabolites of strains X-33 and hSOD. Concentrations of residual glucose, arabitol, pyruvate, acetaldehyde, ethanol and acetate were measured in shake flasks at two time points: at exponential growth (striped bars) and at a late growth phase (filled bars). Error bars indicate standard errors of the mean of two parallel cultures.

metabolism on protein production could be reproduced, indicating a broader validity of the approach discussed here (data not shown).

3.5. Intracellular fluxes and extracellular metabolites of mutant strains

Residual glucose and extracellular metabolites (pyruvate, acetaldehyde, ethanol, acetate and arabitol) were measured in batch cultures of the wild-type and the hSOD strain, and all mutants during exponential growth (same as for ^{13}C labeling) and at a late growth phase. Only minor differences were observed between the wild-type and the hSOD strain (Fig. 5). In line with the predicted flux changes, ethanol and arabitol concentrations were lower in supernatants of the production strain while secreted acetate was increased at the late growth phase. It should be noted that extracellular acetate and also acetaldehyde concentrations were below the detection limit during exponential growth in all strains. Overexpression of PPP genes had minor impact on extracellular metabolites (Fig. 6), except for *GND2*, reducing acetaldehyde, ethanol and acetate in the supernatant. *GDH3* had no significant impact on extracellular metabolites, while *MDH1* overexpression reduced ethanol and acetate secretion. Deletions in the fermentative pathway led to the accumulation of upstream metabolites, and in case of Δ*pdc1* acetaldehyde and ethanol were not produced at all (Fig. 6). Both Δ*adh2* and Δ*ald4* did not abolish the respective production of ethanol and acetate. The alcohol dehydrogenase genes of *P. pastoris* have not yet been clearly annotated according to their biochemical function, indicating that more than one knockout is necessary to eliminate ethanol formation. Similarly, *Ald4* may not be the only enzyme responsible for acetaldehyde oxidation. Moreover, Δ*ald4* led to a 2-fold increase in ethanol production, probably by channeling the acetaldehyde overflow. This strong increase in ethanol production may explain that Δ*ald4* did not improve hSOD production as predicted. It needs to be evaluated in future if an attenuation or knockout of both reactions is needed to increase recombinant protein production. The intracellular flux distribution of the mutant strains (data not shown) was measured, but no statistically significant changes compared to the flux distribution of the SOD strain were obtained. As fluxes in the hSOD strain already changed toward the direction in which the mutants would be attained we assume that further significant flux changes need additional metabolic engineering of the production

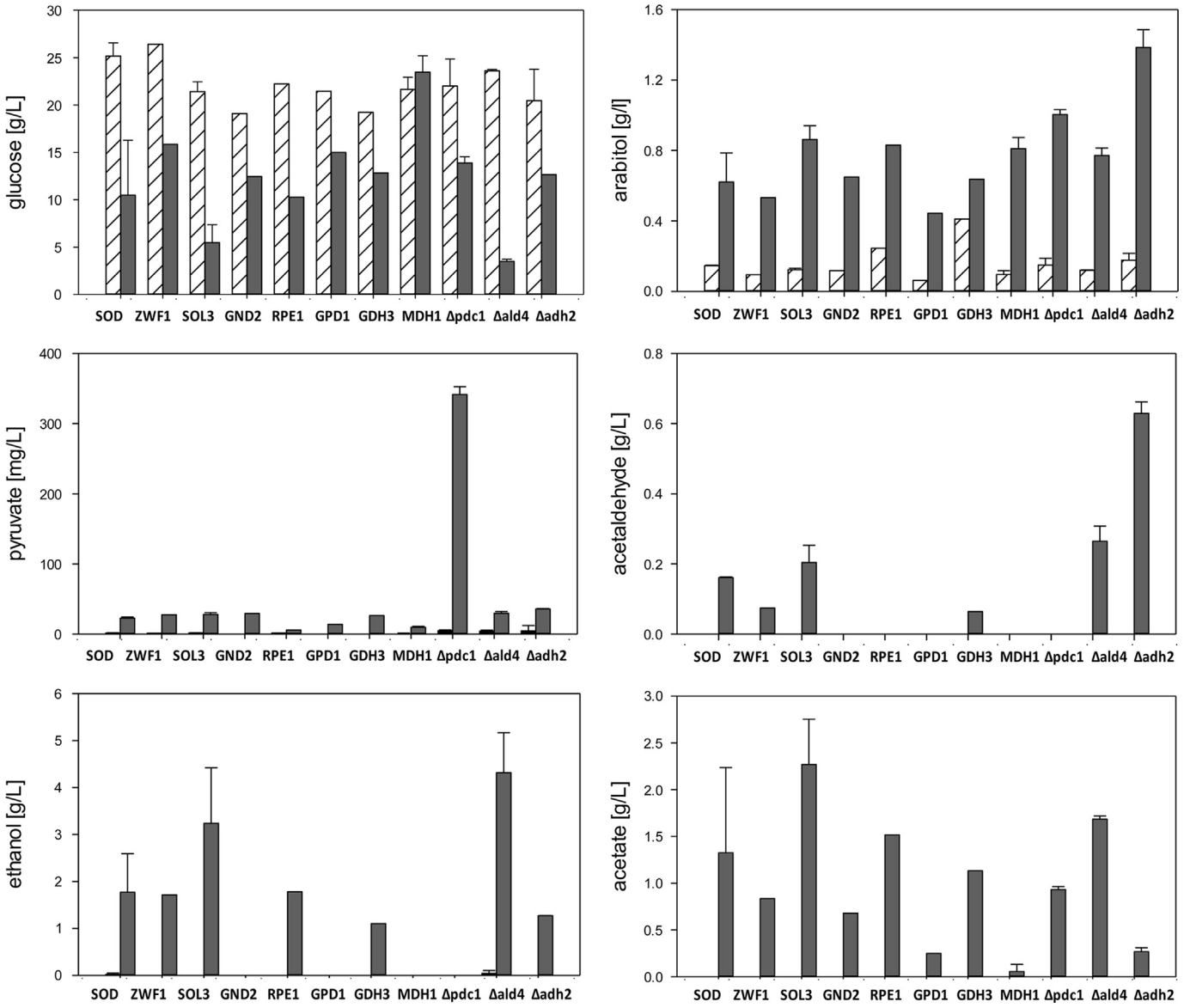

Fig. 6. Extracellular metabolites of mutant strains, compared to the parental control strain hSOD. Data are derived and displayed as described for fig. 6.

host. The total NADP/H pool and the anabolic reduction charge were unchanged in the *ZWF1* strain compared to the hSOD strain (but still threefold more reduced than in the wild type strain). Surprisingly the NADP/H system was more oxidized in the *SOL3* strain than in the hSOD parent strain (Table 1) while *SOL3* overexpression had a strong positive impact on hSOD production. This has been observed consistently in several measurements and may lead to the conclusion that the impact of PPP may go beyond the provision of reduced equivalents.

4. Conclusions

We could demonstrate that recombinant protein production in *P. pastoris* causes significant flux changes which could be reconstructed by a GEM with high accuracy. MOMA and FSEOF turned out as efficient tools to predict which gene knockouts or overexpressions may improve production of a recombinant protein. About 70% of the predicted beneficial mutations were already anticipated by flux changes in the same direction the non-mutated hSOD overproduction strain compared to the wild type. Obviously regulatory plasticity of the yeast metabolism directs fluxes towards what is needed for recombinant protein production. Five out of 9 tested single gene modifications (overexpression or knockout) led to a significant improvement of recombinant protein production, indicating the benefit of a further shift of these pathways. A further positive effect of combined modifications may be anticipated, especially of consecutive steps of the PPP. This work is currently in progress in our laboratory.

Metabolic models provide the power to describe catabolic and anabolic processes of cellular growth and product formation. Prediction of metabolic engineering targets was applied successfully to enhance production of metabolites, such as ethanol (Bro et al., 2006), succinate (Kim et al., 2007), lysine (Becker et al., 2011), sesquiterpenes (Asadollahi et al., 2009), or polyhydroxyalkanoates (Poblete-Castro et al., 2013). Obviously model based metabolic engineering works successfully not only for products of the primary metabolism, but also for secondary metabolites as well as for biopolymers including proteins.

Metabolic models also consider the demand of energy and reductive power for the synthesis of biomass and even complex products like recombinant proteins. The protein secretion process, however, adds further complexity. Chaperone activity consumes ATP in multiple cycles of binding and release of a folding polypeptide (Walter and Buchner, 2002) which cannot be described stoichiometrically. Similarly, the demand of NADPH for redox balancing of oxidative protein folding is not stoichiometrically coupled to the number of disulfide bonds to be closed (Margittai and Sitia, 2011). To exclude this complexity in this work we have focused on non-secreted proteins. First attempts to model the secretory pathway of yeast have been described by Feizi et al. (2013) and will pave the way towards integration of secretion into the reconstruction of protein production.

Conflict of interest

The authors declare no financial or commercial conflict of interest.

Acknowledgments

This work was funded by the Austrian Science Fund (FWF): Doctoral Program BioToP—Biomolecular Technology of Proteins (FWF W1224). Further support by the Federal Ministry of Science, Research and Economy (BMWFW), the Federal Ministry of Traffic, Innovation and Technology (bmvit), the Styrian Business Promotion Agency SFG, the Standortagentur Tirol and ZIT – Technology Agency of the City of Vienna through the COMET-Funding Program managed by the Austrian Research Promotion Agency FFG is acknowledged. EQ BOKU VIBT GmbH is acknowledged for providing mass spectrometry instrumentation. This work was also supported by the Technology Development Program to Solve Climate Changes on Systems Metabolic Engineering for Biorefineries (NRF-2012-C1AAA001-2012M1A2A2026556) from the Ministry of Education, Science and Technology through the National Research Foundation of Korea. The authors thank Stefanie Müller for her excellent technical assistance.

Appendix A. Supplementary material

Supplementary data associated with this article can be found in the online version at http://dx.doi.org/10.1016/j.ymben.2014.05.011.

References

Asadollahi, M.A., Maury, J., Patil, K.R., Schalk, M., Clark, A., Nielsen, J., 2009. Enhancing sesquiterpene production in *Saccharomyces cerevisiae* through in silico driven metabolic engineering. Metab. Eng. 11, 328–334.

Ask, M., Bettiga, M., Duraiswamy, V.R., Olsson, L., 2013. Pulsed addition of HMF and furfural to batch-grown xylose-utilizing *Saccharomyces cerevisiae* results in different physiological responses in glucose and xylose consumption phase. Biotechnol. Biofuels 6, 181.

Baumann, K., Carnicer, M., Dragosits, M., Graf, A.B., Stadlmann, J., Jouhten, P., Maaheimo, H., Gasser, B., Albiol, J., Mattanovich, D., Ferrer, P., 2010. A multilevel study of recombinant *Pichia pastoris* in different oxygen conditions. BMC Syst. Biol. 4, 141.

Becker, J., Zelder, O., Häfner, S., Schroder, H., Wittmann, C., 2011. From zero to hero: design-based systems metabolic engineering of *Corynebacterium glutamicum* for L-lysine production. Metab. Eng. 13, 159–168.

Blumhoff, M., Steiger, M.G., Marx, H., Mattanovich, D., Sauer, M., 2013. Six novel constitutive promoters for metabolic engineering of *Aspergillus niger*. Appl. Microbiol. Biotechnol. 97, 259–267.

Bro, C., Regenberg, B., Forster, J., Nielsen, J., 2006. *In silico* aided metabolic engineering of *Saccharomyces cerevisiae* for improved bioethanol production. Metab. Eng. 8, 102–111.

Canelas, A.B., ten Pierick, A., Ras, C., Seifar, R.M., van Dam, J.C., van Gulik, W.M., Heijnen, J.J., 2009. Quantitative evaluation of intracellular metabolite extraction techniques for yeast metabolomics. Anal. Chem. 81, 7379–7389.

Carnicer, M., Baumann, K., Toplitz, I., Sánchez-Ferrando, F., Mattanovich, D., Ferrer, P., Albiol, J., 2009. Macromolecular and elemental composition analysis and extracellular metabolite balances of *Pichia pastoris* growing at different oxygen levels. Microb. Cell Fact. 8, 65.

Caspeta, L., Shoaie, S., Agren, R., Nookaew, I., Nielsen, J., 2012. Genome-scale metabolic reconstructions of *Pichia stipitis* and *Pichia pastoris* and *in silico* evaluation of their potentials. BMC Syst. Biol. 6, 24.

Castelli, L.M., Lui, J., Campbell, S.G., Rowe, W., Zeef, L.A., Holmes, L.E., Hoyle, N.P., Bone, J., Selley, J.N., Sims, P.F., Ashe, M.P., 2011. Glucose depletion inhibits translation initiation via eIF4A loss and subsequent 48S preinitiation complex accumulation, while the pentose phosphate pathway is coordinately upregulated. Mol. Biol. Cell. 22, 3379–3393.

Choi, H.S., Lee, S.Y., Kim, T.Y., Woo, H.M., 2010. *In silico* identification of gene amplification targets for improvement of lycopene production. Appl. Environ. Microbiol. 76, 3097–3105.

Chung, B.K., Selvarasu, S., Andrea, C., Ryu, J., Lee, H., Ahn, J., Lee, D.Y., 2010. Genome-scale metabolic reconstruction and in silico analysis of methylotrophic yeast *Pichia pastoris* for strain improvement. Microb. Cell Fact. 9, 50.

Damasceno, L.M., Huang, C.J., Batt, C.A., 2012. Protein secretion in *Pichia pastoris* and advances in protein production. Appl. Microbiol. Biotechnol. 93, 31–39.

De Schutter, K., Lin, Y.C., Tiels, P., Van Hecke, A., Glinka, S., Weber-Lehmann, J., Rouzé, P., Van de Peer, Y., Callewaert, N., 2009. Genome sequence of the recombinant protein production host *Pichia pastoris*. Nat. Biotechnol. 27, 561–566.

Dragosits, M., Stadlmann, J., Albiol, J., Baumann, K., Maurer, M., Gasser, B., Sauer, M., Altmann, F., Ferrer, P., Mattanovich, D., 2009. The effect of temperature on the proteome of recombinant *Pichia pastoris*. J. Proteome Res. 8, 1380–1392.

Driouch, H., Melzer, G., Wittmann, C., 2012. Integration of *in vivo* and *in silico* metabolic fluxes for improvement of recombinant protein production. Metab. Eng. 14, 47–58.

Feizi, A., Österlund, T., Petranovic, D., Bordel, S., Nielsen, J., 2013. Genome-scale modeling of the protein secretory machinery in yeast. PLoS One 8, e63284.

Fell, D.A., 1998. Increasing the flux in metabolic pathways: a metabolic control analysis perspective. Biotechnol. Bioeng. 58, 121–124.

Gasser, B., Prielhofer, R., Marx, H., Maurer, M., Nocon, J., Steiger, M., Puxbaum, V., Sauer, M., Mattanovich, D., 2013. *Pichia pastoris*: protein production host and model organism for biomedical research. Future Microbiol. 8, 191–208.

Gonzalez, R., Andrews, B.A., Molitor, J., Asenjo, J.A., 2003. Metabolic analysis of the synthesis of high levels of intracellular human SOD in *Saccharomyces cerevisiae* rhSOD 2060 411 SGA122. Biotechnol. Bioeng. 82, 152–169.

Heiss, S., Maurer, M., Hahn, R., Mattanovich, D., Gasser, B., 2013. Identification and deletion of the major secreted protein of *Pichia pastoris*. Appl. Microbiol. Biotechnol. 97, 1241–1249.

Heyland, J., Blank, L.M., Schmid, A., 2011a. Quantification of metabolic limitations during recombinant protein production in *Escherichia coli*. J. Biotechnol. 155, 178–184.

Heyland, J., Fu, J., Blank, L.M., Schmid, A., 2010. Quantitative physiology of *Pichia pastoris* during glucose-limited high-cell density fed-batch cultivation for recombinant protein production. Biotechnol. Bioeng. 107, 357–368.

Heyland, J., Fu, J., Blank, L.M., Schmid, A., 2011b. Carbon metabolism limits recombinant protein production in *Pichia pastoris*. Biotechnol. Bioeng. 108, 1942–1953.

Idiris, A., Tohda, H., Kumagai, H., Takegawa, K., 2010. Engineering of protein secretion in yeast: strategies and impact on protein production. Appl. Microbiol. Biotechnol. 86, 403–417.

Jefferson, R.A., Burgess, S.M., Hirsh, D., 1986. beta-glucuronidase from *Escherichia coli* as a gene-fusion marker. Proc. Natl. Acad. Sci. USA 83, 8447–8451.

Jordà, J., Jouhten, P., Cámara, E., Maaheimo, H., Albiol, J., Ferrer, P., 2012. Metabolic flux profiling of recombinant protein secreting *Pichia pastoris* growing on glucose:methanol mixtures. Microb. Cell Fact. 11, 57.

Kaleta, C., Schäuble, S., Rinas, U., Schuster, S., 2013. Metabolic costs of amino acid and protein production in *Escherichia coli*. Biotechnol. J. 8, 1105–1114.

Kazemi Seresht, A., Cruz, A.L., de Hulster, E., Hebly, M., Palmqvist, E.A., van Gulik, W., Daran, J.M., Pronk, J., Olsson, L., 2013. Long-term adaptation of *Saccharomyces cerevisiae* to the burden of recombinant insulin production. Biotechnol. Bioeng. 110, 2749–2763.

Kim, H.J., Kwon, Y.D., Lee, S.Y., Kim, P., 2012. An engineered *Escherichia coli* having a high intracellular level of ATP and enhanced recombinant protein production. Appl. Microbiol. Biotechnol. 94, 1079–1086.

Kim, T.Y., Kim, H.U., Park, J.M., Song, H., Kim, J.S., Lee, S.Y., 2007. Genome-scale analysis of *Mannheimia succiniciproducens* metabolism. Biotechnol. Bioeng. 97, 657–671.

Klein, T., Lange, S., Wilhelm, N., Bureik, M., Yang, T.H., Heinzle, E., Schneider, K., 2014. Overcoming the metabolic burden of protein secretion in *Schizosaccharomyces pombe*: a quantitative approach using ^{13}C-based metabolic flux analysis. Metab. Eng. 21, 34–45.

Krüger, A., Grüning, N.M., Wamelink, M.M., Kerick, M., Kirpy, A., Parkhomchuk, D., Bluemlein, K., Schweiger, M.R., Soldatov, A., Lehrach, H., Jakobs, C., Ralser, M., 2011. The pentose phosphate pathway is a metabolic redox sensor and regulates transcription during the antioxidant response. Antioxid. Redox Signal. 15, 311–324.

Margittai, E., Sitia, R., 2011. Oxidative protein folding in the secretory pathway and redox signaling across compartments and cells. Traffic 12, 1–8.

Marx, H., Mecklenbräuker, A., Gasser, B., Sauer, M., Mattanovich, D., 2009. Directed gene copy number amplification in *Pichia pastoris* by vector integration into the ribosomal DNA locus. FEMS Yeast Res. 9, 1260–1270.

Mattanovich, D., Callewaert, N., Rouzé, P., Lin, Y.C., Graf, A., Redl, A., Tiels, P., Gasser, B., De Schutter, K., 2009. Open access to sequence: browsing the *Pichia pastoris* genome. Microb. Cell Fact. 8, 53.

McAlister-Henn, L., Thompson, L.M., 1987. Isolation and expression of the gene encoding yeast mitochondrial malate dehydrogenase. J. Bacteriol. 169, 5157–5166.

Messiha, H., Kent, E., Malys, N., Carroll, K., Swainston, N., Mendes, P., Smallbone, K., 2009. Enzyme characterisation and kinetic modelling of the pentose phosphate pathway in yeast:PeerJ PrePrints vol 2,e146v4 2014.

Oddone, G.M., Mills, D.A., Block, D.E., 2009. A dynamic, genome-scale flux model of *Lactococcus lactis* to increase specific recombinant protein expression. Metab. Eng. 11, 367–381.

Ortmayr, K., Nocon, J., Gasser, B., Mattanovich, D., Hann, S., Kollensperger, G., 2014. Sample preparation workflow for the LC-MS based analysis of $NADP^+$ and NADPH in yeast. J. Sep. Sci., http://dx.doi.org/10.1002/jssc.201400290.

Pedersen, H., Carlsen, M., Nielsen, J., 1999. Identification of enzymes and quantification of metabolic fluxes in the wild type and in a recombinant *Aspergillus oryzae* strain. Appl. Environ. Microbiol. 65, 11–19.

Pfeffer, M., Maurer, M., Kollensperger, G., Hann, S., Graf, A.B., Mattanovich, D., 2011. Modeling and measuring intracellular fluxes of secreted recombinant protein in *Pichia pastoris* with a novel 34S labeling procedure. Microb. Cell Fact. 10, 47.

Pflügl, S., Marx, H., Mattanovich, D., Sauer, M., 2012. 1,3-Propanediol production from glycerol with *Lactobacillus diolivorans*. Bioresour. Technol. 119, 133–140.

Poblete-Castro, I., Binger, D., Rodrigues, A., Becker, J., Martins Dos Santos, V.A., Wittmann, C., 2013. *In-silico*-driven metabolic engineering of *Pseudomonas putida* for enhanced production of poly-hydroxyalkanoates. Metab. Eng. 15, 113–123.

Porro, D., Gasser, B., Fossati, T., Maurer, M., Branduardi, P., Sauer, M., Mattanovich, D., 2011. Production of recombinant proteins and metabolites in yeasts: when are these systems better than bacterial production systems? Appl. Microbiol. Biotechnol. 89, 939–948.

Quek, L.E., Wittmann, C., Nielsen, L.K., Kromer, J.O., 2009. OpenFLUX: efficient modelling software for ^{13}C-based metabolic flux analysis. Microb. Cell Fact. 8, 25.

Segrè, D., Vitkup, D., Church, G.M., 2002. Analysis of optimality in natural and perturbed metabolic networks. Proc. Natl. Acad. Sci. USA 99, 15112–15117.

Sheikholeslami, Z., Jolicoeur, M., Henry, O., 2013. Probing the metabolism of an inducible mammalian expression system using extracellular isotopomer analysis. J. Biotechnol. 164, 469–478.

Sohn, S.B., Graf, A.B., Kim, T.Y., Gasser, B., Maurer, M., Ferrer, P., Mattanovich, D., Lee, S.Y., 2010. Genome-scale metabolic model of methylotrophic yeast *Pichia pastoris* and its use for in silico analysis of heterologous protein production. Biotechnol. J. 5, 705–715.

Souza, M.A., Ribeiro, M.Z., Silva, D.P., Pessoa, A., Vitolo, M., 2002. Effect of pH on the stability of hexokinase and glucose 6-phosphate dehydrogenase. Appl. Biochem. Biotechnol. 98-100, 265–272.

Stadlmayr, G., Mecklenbräuker, A., Rothmüller, M., Maurer, M., Sauer, M., Mattanovich, D., Gasser, B., 2010. Identification and characterisation of novel *Pichia pastoris* promoters for heterologous protein production. J. Biotechnol. 150, 519–529.

Vijayasankaran, N., Carlson, R., Srienc, F., 2005. Metabolic pathway structures for recombinant protein synthesis in *Escherichia coli*. Appl. Microbiol. Biotechnol. 68, 737–746.

Walter, S., Buchner, J., 2002. Molecular chaperones: cellular machines for protein folding. Angew. Chem. Int. Ed. Engl. 41, 1098–1113.

Weber, J., Hoffmann, F., Rinas, U., 2002. Metabolic adaptation of *Escherichia coli* during temperature-induced recombinant protein production: 2. Redirection of metabolic fluxes. Biotechnol. Bioeng. 80, 320–330.

Wittmann, C., Weber, J., Betiku, E., Kromer, J., Bohm, D., Rinas, U., 2007. Response of fluxome and metabolome to temperature-induced recombinant protein synthesis in *Escherichia coli*. J. Biotechnol. 132, 375–384.

Xu, C., Liu, L., Zhang, Z., Jin, D., Qiu, J., Chen, M., 2013. Genome-scale metabolic model in guiding metabolic engineering of microbial improvement. Appl. Microbiol. Biotechnol. 97, 519–539.

Zamboni, N., Fendt, S.M., Rühl, M., Sauer, U., 2009. (13)C-based metabolic flux analysis. Nat. Protoc. 4, 878–892.

Zamboni, N., Fischer, E., Sauer, U., 2005. FiatFlux—a software for metabolic flux analysis from ^{13}C-glucose experiments. BMC Bioinform. 6, 209.

Zampar, G.G., Kümmel, A., Ewald, J., Jol, S., Niebel, B., Picotti, P., Aebersold, R., Sauer, U., Zamboni, N., Heinemann, M., 2013. Temporal system-level organization of the switch from glycolytic to gluconeogenic operation in yeast. Mol. Syst. Biol., 9; p. 651.

Zubay, G., 1988. Biochemistry. Macmillan, New York.